Introduction to superconducting qubits
USEQIP

Adrian Lupascu

Institute for Quantum Computing
Department of Physics and Astronomy
University of Waterloo, Canada

June 9, 2011

Superconducting qubits among other types of quantum hardware I

Various types of physical systems are presently being investigated as qubits.
A first class of qubits is formed of the "traditional" quantum systems. This class contains physical systems such as single atoms and ions [1], nuclear spins [2], and single photons [3]. The quantum behavior of such systems had already been observed in the laboratory and well understood at the time when the new ideas in quantum computing emerged.

nuclear spins

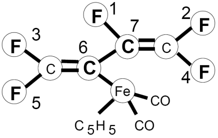

Vandersypen *et al.* Nature **414**, 883 (2001)

photons

O'Brien *et al.* Nature **426**, 264 (2003)

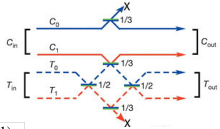

atoms

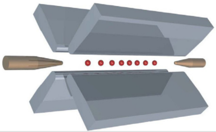

Blatt and Steane, *"Quantum information processing with trapped ions"* (2005)

These quantum systems are well characterized. They have the advantage of long quantum coherence times, which are in general well understood. Their drawback is the difficulty to scale the system up to a large number of qubits.

Superconducting qubits among other types of quantum hardware II

A second class of qubits is formed by "artificial" quantum systems. These are solid state structures, based on semi-conductors or super-conductors, which are patterned at the micrometer scale using modern lithography techniques.

Important features of solid-state qubits:

- large flexibility in design of quantum properties
- the excitation energy is higher than achievable cryogenic temperatures $\Rightarrow$ initialization is easy
- good prospects for scalability
- decoherence related to the solid-state environment is difficult to remove

Review articles: superconducting qubits [4] and quantum dot based qubits [5].

Superconducting qubits among other types of quantum hardware III

solid – state systems

Nakamura *et al.* Nature **398**, 786 (1999)

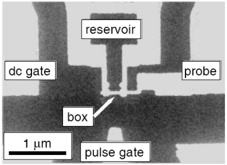

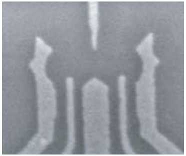

Koppens *et al.* **442**, 766 (2006)

The first demonstration of quantum coherence of a single superconducting qubit dates from 1999 [6]. This field of research is presently quite vast, and it evolved in many directions, some going beyond quantum information processing:

- quantum design issues
- characterization of decoherence
- quantum operations on one and two qubits
- quantum optics in the strong coupling regime (*eg* cQED)

Superconducting qubits among other types of quantum hardware IV

- quantum measurement

The goal of this lecture is to introduce the main physical concepts on which superconducting qubits are based. A specific type of superconducting qubit, the phase qubit, will be described in detail.

Table of contents

The L-C resonator/ I

In (most) superconducting qubits, the lowest excitations are characterized by the dynamics of the electromagnetic fields and of the charges in superconductors at frequencies ω that correspond to free space propagation wavelengths $\lambda = c/\nu$ much longer than the size of the circuit.

This corresponds to the *lumped approximation for electrical circuits*. We analyze a simple (model for a) lumped circuit, namely the *LC resonator*.

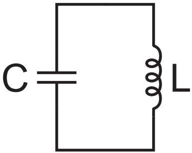

The L-C resonator/ Canonical quantization starting from Kirchhoff's laws I

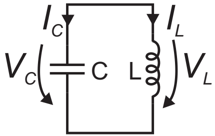

Kirchhoff's laws applied to the LC circuit

- current conservation

$$I_C + I_L = 0 \tag{1}$$

- zero voltage sum

$$V_C - V_L = 0 \tag{2}$$

The L-C resonator/ Canonical quantization starting from Kirchhoff's laws II

It is convenient for later use to describe two-port circuit elements in terms of the *branch flux* Φ_b and *branch charge* Q_b, which are related to the branch voltage V_b and current I_b by

$$Q_b(t) = \int_{-\infty}^{t} I_b(t')dt' \tag{3}$$
$$\Phi_b(t) = \int_{-\infty}^{t} V_b(t')dt'.$$

The relations between flux/charge and current/voltage variables for a capacitor and inductor respectively are:

$$Q_C = CV_C \tag{4}$$
$$I_L = \Phi_L/L.$$

After combining 1,2,3,4 we obtain

$$\frac{d(C\dot{\Phi}_L)}{dt} = -\frac{\Phi_L}{L}. \tag{5}$$

This suggests writing a Lagrangian for the LC resonator

$$\mathcal{L} = \frac{1}{2}C\dot{\Phi}_L^{\,2} - \frac{1}{2}\frac{1}{L}\Phi_L^2, \tag{6}$$

The L-C resonator/ Canonical quantization starting from Kirchhoff's laws III

for which 5 is the Lagrange equation [7]

$$\frac{d}{dt}\left(\frac{d\mathcal{L}}{d\dot{\Phi}_L}\right) = \frac{d\mathcal{L}}{d\Phi_L}. \tag{7}$$

The Lagrangian description of the equation of motion provide a starting point for a *quantum description of the LC circuit* using *canonical quantization*.
The Hamiltonian is expressed in terms of the "coordinate" Φ_L, and the canonically conjugate "momentum" p_{Φ_L}

$$p_{\Phi_L} = \frac{d\mathcal{L}}{d\dot{\Phi}_L} \tag{8}$$

as

$$\mathcal{H}\left(p_{\Phi_L}, \dot{\Phi}_L\right) = p_{\Phi_L}\Phi_L - \mathcal{L} \tag{9}$$

resulting in

$$\mathcal{H}\left(p_{\Phi_L}, \Phi_L\right) = \frac{1}{2}\frac{1}{C}p_{\Phi_L}^2 + \frac{1}{2}\frac{1}{L}\Phi_L^2 \tag{10}$$

The L-C resonator/ Canonical quantization starting from Kirchhoff's laws IV

The procedure for canonical quantization involves the following elements

- Classical Hamiltonian (function of phase space variables) $\Rightarrow$ Quantum Hamiltonian (operator in Hilbert space)

$$\mathcal{H} \rightarrow H$$

- Classical variables $\Rightarrow$ Hermitian operators

$$\Phi_L \rightarrow \mathit{\Phi}$$

$$p_{\Phi_L} \rightarrow p_{\mathit{\Phi}}$$

- Poisson brackets $\Rightarrow$ Commutators

$$\{a, b\} \rightarrow \frac{[a, b]}{i\hbar}$$

The L-C resonator/ Canonical quantization starting from Kirchhoff's laws V

The quantum Hamiltonian of the LC circuit becomes

$$H = \frac{1}{2}\frac{1}{C}p_{\Phi}^2 + \frac{1}{2}\frac{1}{L}\Phi^2 \tag{11}$$

where p_{Φ} and Φ are operators satisfying the commutation relation

$$[p_{\Phi}, \Phi] = i\hbar. \tag{12}$$

The operators p_{Φ} and Φ are analogous to the x and p variables of the familiar harmonic oscillator formed by a mass M attached to a spring of constant k. The correspondence between the variables and the parameters in the two models is:

Harmonic oscillator	**LC resonator**
x	Φ
p	p_{Φ}
M	C
k	L^{-1}

The L-C resonator/ Canonical quantization starting from Kirchhoff's laws VI

The quantum HO is presented in many basic textbooks on quantum mechanics (see *e.g.* [8]). The energy eigenstates of 11 are

$$E_n = (n + 1/2)\,\hbar\omega_{LC}, \tag{13}$$

with

$$\omega_{LC} = 1/\sqrt{LC} \tag{14}$$

(the frequency corresponds to the classical resonance frequency).

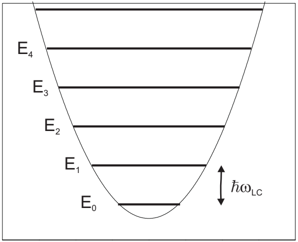

The L-C resonator/ Limitations of standard resonators I

Genuine quantum effects are usually not observed in regular LC circuits, due to thermal population and dissipation.

1. **Thermal population**
   For preparation in the ground state, the temperature T needs to satisfy
   $$k_B T \ll \hbar\omega_{LC}. \tag{15}$$
   This condition is not satisfied for microwave resonators at 300 K. By cooling using a *dilution refrigerator*, temperatures of $T \sim 10$ mK can be attained. Resonators in the microwave range cooled at these temperature are thermalized very effectively. For example $h \times 2\,\mathrm{GHz} = 10 \times k_B \times 10\,\mathrm{mK}$.

The L-C resonator/ Limitations of standard resonators II

2. **Dissipation**
   Normal metal LC resonators with $\omega_{LC} = 2\pi \times (1 - 10)$ GHz have quality factors $Q \sim 10^{1-2} \rightarrow$ *decoherence* sets in fast, over time scales of the order of Q/ω_{LC}.
   Using superconducting materials leads to a large reduction of dissipation:
   $Q_{normal} \sim 10^{1-2} \rightarrow Q_{superconducting} \sim 10^{4-6}$
   In addition, superconductors with Josephson junctions are non-linear $\rightarrow$ anharmonic energy level structure $\rightarrow$ effective two-level system or *quantum bit*

Superconductivity/ Structure of the superconducting state I

Normal state
- finite conductivity
- no electron order
- no energy gap

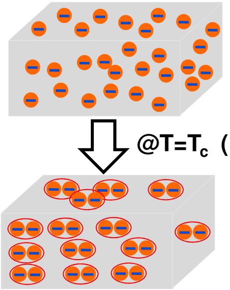

@T=T_c (1.2 K for Aluminum)

Superconducting state
- infinite conductivity
- electron order
- energy gap

The gap for electron-hole excitations survives in small electromagnetic fields.

Lower energy excitations, with anharmonic spectrum → **Josephson energy**, **charging energy**

Superconductivity/ Important properties: no dissipation and phase coherence I

Dissipationless currents The ability to carry a dissipationless current is the most important characteristic of a superconductor. It can be understood by considering the nature of the current carrying states in a superconductor. These states are separated by a significant energy gap from normal-metal-like states in which dissipation is effective. The critical current density of low-temperature superconductors of the order of MA/cm^2, much higher than the currents that are relevant for superconducting qubits.

Phase coherence The wavefunction of superconductors displays phase coherence on a macroscopic scales. Phase gradients are associated with the flow of current. In a bulk superconductor the current density is given by

$$\overrightarrow{J} = \frac{\hbar}{m}\left(\nabla\gamma - \frac{2e}{\hbar}\overrightarrow{A}\right)\rho, \tag{16}$$

where γ is the phase, ρ is the particle density, and $\overrightarrow{A}$ is the vector potential associated with a magnetic field. In this lecture we will not consider the effect of applied magnetic fields, which are important only for multiply connected superconductors, as applicable to *e.g.* the so-called flux qubits.

The Josephson junction/ I

A Josephson junction is a structure formed by two superconducting electrodes separated by a thin tunnel barrier.

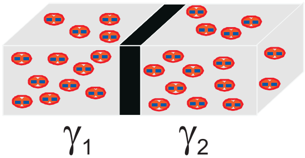

Transport of electrical charge through the barrier takes place through quantum tunneling. The remarkable property of the Josephson junction is the flow of current without dissipation, which is due to tunneling of Cooper pairs through the barrier.

The phase difference $\delta = \gamma_1 - \gamma_2$ is the important variable characterizing the junction. In 1962, Josephson discovered the relations between the phase difference and the current and voltage across the junction. These relations form the basis for the description of superconducting circuits with Josephson junctions.

The Josephson junction/ The Josephson relations I

The first Josephson relation (the current-phase relation)

$$I = I_c \sin \delta, \tag{17}$$

I_c is the *critical current* of the junction, which depends on the superconducting material, barrier thickness and construction, and is proportional to the barrier surface. For typical junctions used for qubits, made of aluminum with a very thin ($\sim$ nm) barrier, and surface ranging from 100x100 nm^2 to 1x1 μm^2, $I_c = 0.1 \div 10\,\mu$A.

The second Josephson relation (the AC Josephson effect)

$$V = \frac{\Phi_0}{2\pi}\frac{d\delta}{dt}, \tag{18}$$

This equation introduces an important constant, the flux quantum Φ_0, which is dual to the Cooper pair charge $2e$. It is given by

$$\Phi_0 = \frac{h}{2e}, \tag{19}$$

which equals 2.067x10^{-15} Wb.

The Josephson junction/ Inductive behavior I

From the 2nd Josephson relation (18) and the definition of the branch flux, we find that

$$\delta = 2\pi \frac{\Phi}{\Phi_0}. \tag{20}$$

Using the 1st Josephson relation (17):

$$I = I_c \sin 2\pi \frac{\Phi}{\Phi_0}. \tag{21}$$

We introduce a new parameter, the *Josephson inductance*:

$$L_J = \frac{\Phi_0}{2\pi I_c}. \tag{22}$$

Including this definition in 21

$$I = \frac{\Phi_0}{2\pi L_J} \sin 2\pi \frac{\Phi}{\Phi_0}. \tag{23}$$

The relation above is similar to 4. In general, a relation of the type $I = I(\Phi)$ corresponds to an inductor. In the limit $|\Phi/\Phi_0| \ll 1$

$$I \simeq \frac{\Phi}{L_J}, \tag{24}$$

The Josephson junction/ Inductive behavior II

and the Josephson junction behaves like a *linear* inductor. For arbitrary values of Φ *the inductance is non-linear*.

For typical Josephson junctions used in qubit circuits: $L_J = 0.03 \div 3$ nH.

The Josephson junction/ Charging energy I

The Josephson relations correctly describe JJs the current flowing *through the barrier*. A second contribution to the overall current appears due to the accumulation of charge:

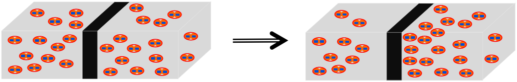

The total current

$$I = I_J + I_C, \tag{25}$$

with I_J given by 23 and $I_C$described in terms of a capacitance C:

$$V_C = \frac{Q_c}{C} \tag{26}$$
$$Q(t) = \int_{-\infty}^{t} I(t')dt'.$$

The Josephson junction/ Josephson junction vs LC resonator I

For an isolated junction the total current $I = 0$, so 25 is equivalent to 1. Therefore, all the relations used to derive the dynamics of the LC resonators (Kirchhoff's laws, and relations between flux/charge and voltage/current) remain unchanged, except for the current-flux relation 4 which is replaced by 23.

The Josephson junction is described by the L_J-C model, analogous to the LC resonator:

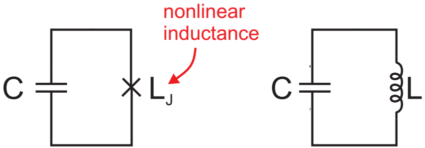

Using the steps that led from 1, 2, 3, and 4 to 11, we can find the quantum Hamiltonian of the Josephson junction

$$H = \frac{1}{2}\frac{1}{C}p_{\Phi}^2 + \frac{(\Phi_0/(2\pi))^2}{L_J}\left(1 - \cos 2\pi\frac{\Phi}{\Phi_0}\right) \tag{27}$$

The Josephson junction/ Energy level structure: anharmonicity I

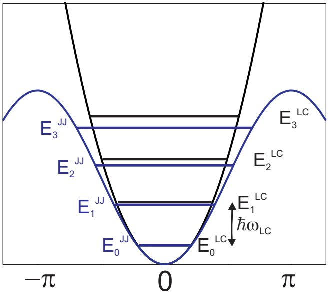

Comparison between energy levels of the Josephson junction and the LC resonator

- $E_n^{JJ} \leq E_n^{LC}$, due to the "softer" potential
- $\left(E_{n+2}^{JJ} - E_{n+1}^{JJ}\right) < \left(E_{n+1}^{JJ} - E_n^{JJ}\right)$, *anharmonic energy level structure*

The phase qubit/ Circuit I

The **phase qubit** is a single Josephson junction, to which a controllable current source is added. It is the smallest quantum superconducting circuit useful as a qubit; for this reason it is used here to explain the following basic concepts: qubit design, intitialization, single and two-qubit control, and measurement. The phase qubit is one of the main candidates for superconducting quantum computing implementation.

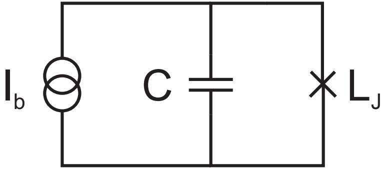

The role of the added current source

- augmentation of anharmonicity
- control of the quantum state

The phase qubit/ "Mesoscopic" Hamiltonian I

The classical description of the phase qubit circuit involves the modification of the Kirchhoff current law for a single junction by the addition of a *bias current* I_b. Eq. 25 is thus used

$$I_J + I_C = I_b. \tag{28}$$

By using the Kirchhoff laws and the appropriate branch relations, we obtain the classical equation of motion

$$\frac{d(C\dot{\Phi})}{dt} = I_b - \frac{\Phi_0}{2\pi L_J} \sin\left(2\pi \frac{\Phi}{\Phi_0}\right). \tag{29}$$

The potential energy is the *tilted washboard potential*

$$\mathcal{U}(\Phi) = -I_b\Phi + \frac{1}{2}\left(\frac{\Phi_0}{2\pi}\right)^2 \frac{1}{L_J}\left(1 - \cos\left(2\pi\frac{\Phi}{\Phi_0}\right)\right). \tag{30}$$

Eq. 29 can be used to build a Lagrangian (see 7) and finally leads to the *mesoscopic* quantum Hamiltonian for the phase qubit

$$H = \frac{1}{2}\frac{1}{C}p_{\Phi}^2 + \frac{\Phi_0^2}{(2\pi)^2 L_J}\left(1 - \cos 2\pi\frac{\Phi}{\Phi_0}\right) - I_b\Phi \tag{31}$$

The phase qubit/ Two-state system approximation I

Consider a fixed bias current $I_{b0} \lesssim I_c$. For typical phase qubits, with $I_c \sim 10\mu$A and $C \sim 10$ fF, the bias current is $I_{b0} \simeq 99\% I_c$. In this situation, typically two-three levels are present in the potential well.

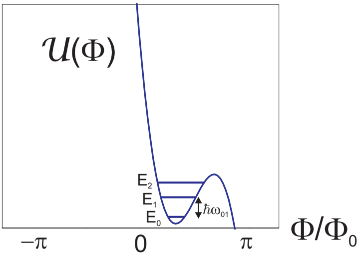

The qubit is the truncation of the Hilbert space to the subspace formed by the ground state $|0\rangle$ and the excited state $|1\rangle$. Note that both the states $|0\rangle$ and $|1\rangle$, and the energy eigenvalues E_0 and E_1 depend on the bias current I_b. It is assumed that they are defined at $I_b = I_{b0}$.

The phase qubit/ Two-state system approximation II

The (controlled) physical evolution has to be such that the system quantum state remains at all times in the *computational subspace*, spanned by the energy eigenstates $|0\rangle$ and $|1\rangle$.
The qubit Hamiltonian (at $I_b = I_{b0}$) is given by

$$H_0 = \frac{\hbar\omega_{01}}{2} Z, \tag{32}$$

where Z is one of the three Pauli matrices

$$X = \begin{bmatrix} 0 & 1 \\ 1 & 0 \end{bmatrix}, \tag{33}$$

$$Y = \begin{bmatrix} 0 & -i \\ i & 0 \end{bmatrix}, \tag{34}$$

$$Z = \begin{bmatrix} 1 & 0 \\ 0 & -1 \end{bmatrix}. \tag{35}$$

For a bias current $I_b = I_{b0} + \delta I_b$, the Hamiltonian is

$$\widetilde{H}(\delta I_b) = H_0 + H(I_{b0} + \delta I_b) - H(I_{b0}). \tag{36}$$

Using 31

$$\widetilde{H}(\delta I_b) = H_0 - \delta I_b \Phi. \tag{37}$$

The phase qubit/ Two-state system approximation III

The control term can be written like

$$-\delta I_b \Phi = -\delta I_b Tr(X\Phi)/2 \times X - \delta I_b Tr(Z\Phi)/2 \times Z. \tag{38}$$

The phase qubit/ Quantum state initialization I

After setting I_b to I_{b0}, a waiting time is allowed for energy relaxation. Due to the typical energy levels splitting ($\tilde{1}0$ GHz) being much larger that the thermal energy (25 mK, which corresponds to 0.5 GHz is common in a dilution refrigerator), the ground state is prepared with large fidelity. State fidelity can be improved using cooling. Two methods possible:

- set a bias corresponding to large energy level splitting E_{ge}^{prep} (much larger than $k_B T$), then change bias to operation setting E_{ge}^{op} [9]
- use cooling methods similar to atomic physics (eg pumping, see [10])

Note: these methods are more suitable for other types of superconducting qubits (*eg* the flux qubit).
State preparation time can be reduced to times $\ll$ relaxation time by using a fast reset mechanism [11].

The phase qubit/ Quantum state control I

Single qubits

The availability of the terms X and Z provides the means for *arbitrary single qubit operations*. To understand this, one can use a transformation to the rotation frame. Define the rotating frame

$$|\tilde{\Psi}(t)> = U_f^\dagger(t)|\Psi(t)> \tag{39}$$

with

$$U_f^\dagger(t) = e^{iH_0 t/\hbar} \tag{40}$$

with $|\Psi(t)>$ the qubit wavefunction in the Schrodinger representation. Without control ($\delta I_b = 0$): $|0>$ and $|1>$ are stationary (no phase factors). With control

$$i\frac{d}{dt}|\tilde{\Psi}(t)> = \tilde{H}_f(t)|\tilde{\Psi}(t)> \tag{41}$$

with

$$\tilde{H}_f(t) = U_f^\dagger(t)(H_0 + \delta H(t))U_f(t) - i\hbar U_f^\dagger(t)\frac{dU_f(t)}{dt}, \tag{42}$$

leading to

$$\tilde{H}_f(t) = U_f^\dagger(t)\delta H(t)U_f(t). \tag{43}$$

Phase gates (rotations around z axis)

The phase qubit/ Quantum state control II

Slow changes in δI_b:

$$U_f^\dagger(t)(Z)U_f(t) = Z, \tag{44}$$

which leads to a phase gate, with the total rotation angle determined by the change in the current. Note that terms proportional to X exist. For slow enough variation the evolution is adiabatic: as long as $\delta I_b = 0$ at the end of the pulse, the only result is the accumulation of phase factors.

Rotations around an axis in the xy plane

Consider the *ac* modulation of δI_b, leading to

$$-\delta I_b Tr(X\Phi)/2 = A\cos(\omega_{01}t + \phi), \tag{45}$$

with ϕ the driving phase and A the amplitude, proportional to the amplitude of the δI_b fluctuations. So

$$U_f^\dagger(t)(A\cos(\omega_{01}t+\phi)X)U_f(t) = \cos(\omega_{01}t+\phi)\left(\cos(\omega_{01}t)X - \sin(\omega_{01}t)Y\right). \tag{46}$$

The fast oscillating terms can be dropped (the rotating wave approximation) which leads to

$$U_f^\dagger(t)(A\cos(\omega_{01}t+\phi)X)U_f(t) \approx \cos\phi X - \sin\phi Y. \tag{47}$$

The phase qubit/ Quantum state control III

Based on this rotations around any axis in the *xy* plane of the Bloch sphere can be implemented. Note that fast changes result in a contribution to the Hamiltonian in the rotating frame which is proportional with Z; this is negligible for small driving amplitudes. In

The phase qubit/ Quantum state control IV

Steffen *et al* [12] the procedure to control and characterize the state of a phase qubit is described.

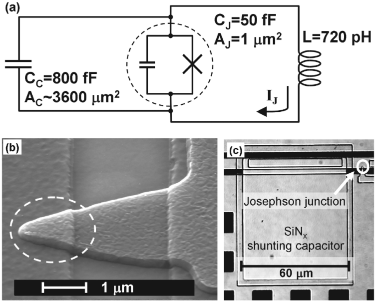

FIG. 2. Circuit diagram and micrograph of the redesigned phase qubit. (a) A small-area ($A_J \sim 1\ \mu m^2$) Josephson junction with little self-capacitance ($C_J = 50$ fF) is shunted by a large ($A_C \sim 3600\ \mu m^2$) high quality capacitor with $C_C = 800$ fF. The qubit bias current I_J is induced through an inductor with $L = 720\ p$H. (b) A scanning electron microscope image of the small-area Josephson junction shows well-defined features at submicron length scales. (c) An optical image of the shunting capacitor and the Josephson junction (white circle).

The phase qubit/ Quantum state control V

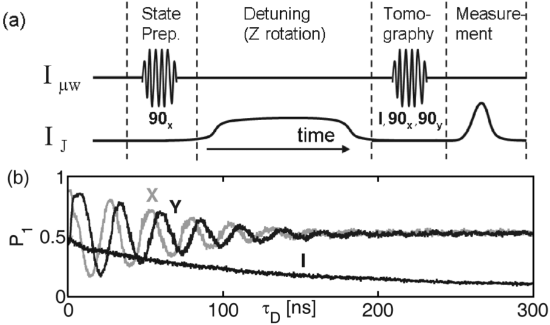

The phase qubit/ Quantum state measurement I

Measurement of the quantum state proceeds in two steps.

- The bias I_b is increase from I_{b0} to $I_{b,readout}$ *adiabatically* $\rightarrow$ the probability of occupation for each energy eigenstates is not changed
- After a suitable waiting time: quantum tunneling takes place *if the qubit was in state* $|1\rangle$ and does not take place *if the qubit was in state* $|0\rangle$. For superpositions of $|0\rangle$ and $|1\rangle$, the probability of no-tunneling/tunneling is given by the probabilities of the respective corresponding eigenstate. A tunneling event produces an avalanche effect which can be easily detected by electrical means.

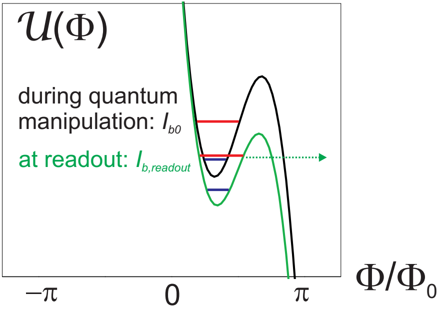

The phase qubit/ Quantum state measurement II

This is a result from an experiment in 2008 [14]

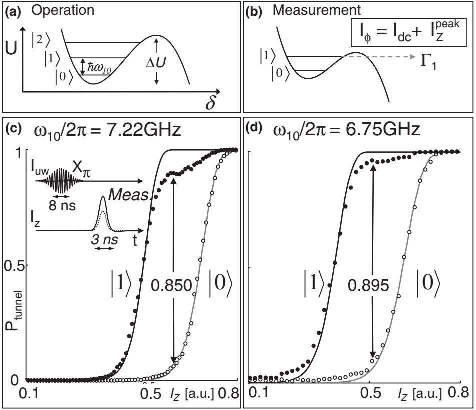

The phase qubit/ Quantum state measurement III

Note:

1. readout based on tunneling is particularly convenient for phase qubits, as a metastable potential is available as part of the qubit biasing circuit
2. a large variety of readout schemes exist
3. some readout schemes, such as based on circuit quantum electrodynamics [15], are generic and applicable to most types of qubits

References I

Garcia-Ripoll, J. J., Zoller, P., and Cirac, J. I.
Journal of Physics B: Atomic, Molecular and Optical Physics **38**(9), S567–S578 (2005).

Vandersypen, L. M. K., Steffen, M., Breyta, G., Yannoni, C. S., Sherwood, M. H., and Chuang, I. L.
Nature **414**, 883 (2001).

J. L. O'Brien, G. J. Pryde, A. G. W. T. C. R. and Branning, D.
Nature **426**, 264 (2003).

Clarke, J. and Wilhelm, F. K.
Nature **453**, 1031 (2008).

Loss, D. and DiVincenzo, D.
Phys. Rev. A **57**(1), 120 January (1998).

Nakamura, Y., Pashkin, Y. A., and Tsai, J. S.
Nature **398**, 786 (1999).

References II

Goldstein, H., Poole, C., and Safko, J.
Classical mechanics.
Classical mechanics (3rd ed.) by H. Goldstein, C. Poolo, and J. Safko. San Francisco: Addison-Wesley, 2002., (2002).

Cohen-Tannoudji, C., Diu, B., and Laloe, F.
Quantum Mechanics, Volume 1.
(1986).

Lupascu, A., Driessen, E. F. C., Roschier, L., Harmans, C. J. P. M., and Mooij, J. E.
Phys. Rev. Lett. **96**(12), 127003 Mar (2006).

Valenzuela, S. O., Oliver, W. D., Berns, D. M., Berggren, K. K., Levitov, L. S., and Orlando, T. P.
Science **314**, 1589 (2006).

M. D. Reed, B. R. Johnson, A. A. H. L. D. J. M. C. D. I. S. L. F. and Schoelkopf, R. J.
Appl. Phys. Lett. **96**, 203110 (2010).

References III

Steffen, M., Ansmann, M., McDermott, R., Katz, N., Bialczak, R. C., Lucero, E., Neeley, M., Weig, E. M., Cleland, A. N., and Martinis, J. M.
Phys Rev Lett **97**(5), 050502 Aug (2006).

McDermott, R., Simmonds, R., Steffen, M., Cooper, K., Cicak, K., Osborn, K., Oh, S., Pappas, D., and Martinis, J.
Science **307**(5713), 1299 August (2003).

Erik Lucero, M. Hofheinz, M. A. R. C. B. N. K. M. N. A. D. O. H. W. A. N. C. and Martinis, J. M.
Physical Review Letters **100**, 247001 (2008).

Blais, A., Huang, R., Wallraff, A., Girvin, S., and Schoelkopf, R.
PHYSICAL REVIEW A Phys Rev A **69**, 062320 (2004).